Journal of Translational Autoimmunity 7 (2023) 100210

Contents lists available at ScienceDirect

Journal of Translational Autoimmunity

journal homepage: www.sciencedirect.com/journal/journal-of-translational-autoimmunity

Metformin-induced activation of Ca^{2+} signaling prevents immune infiltration/pathology in Sjogren's syndrome-prone mouse models

Viviane Nascimento Da Conceicao [a], Yuyang Sun [a], Xiufang Chai [a], Julian L. Ambrus [b], Bibhuti B. Mishra [c], Brij B. Singh [a,*]

[a] Department of Periodontics, School of Dentistry, University of Texas Health Science Center San Antonio, San Antonio, TX 78229, USA
[b] Division of Allergy, Immunology, and Rheumatology, Department of Medicine, School of Medicine and Biomedical Sciences, State University of New York, Buffalo, NY 14203, USA
[c] Department of Developmental Dentistry, School of Dentistry, University of Texas Health Science Center San Antonio, San Antonio, TX 78229, USA

ARTICLE INFO

Handling Editor: Dr Y Renaudineau

Keywords:
Primary Sjogren's syndrome
Ca2+ signaling
Metformin, immune cell activation
ER stress
Alarmins
Salivary gland dysfunction

ABSTRACT

Immune cell infiltration and glandular dysfunction are the hallmarks of autoimmune diseases such as primary Sjogren's syndrome (pSS), however, the mechanism(s) is unknown. Our data show that metformin-treatment induces *Ca2+ signaling that restores saliva secretion and prevents immune cell infiltration in* the salivary glands of IL14α-transgenic mice (IL14α), which is a model for pSS. Mechanistically, we show that loss of *Ca2+ signaling is a major contributing factor, which is restored by metformin treatment,* in IL14α mice. Furthermore, the loss of *Ca2+ signaling leads to ER stress in salivary glands.* Finally, restoration of metformin-induced *Ca2+ signaling* inhibited the release of alarmins and prevented the activation of ER stress that was essential for immune cell infiltration. These results suggest that loss of metformin-mediated activation of *Ca2+* signaling prevents ER stress, which inhibited the release of alarmins that induces immune cell infiltration leading to salivary gland dysfunction observed in pSS.

1. Introduction

Primary sjögren's syndrome (pSS), a well-established chronic systemic autoimmune disease is characterized by intensified lymphocytic infiltration in exocrine glands, and damage of both salivary and lacrimal glands [1]. The most common clinical symptoms are xerophthalmia (dry eyes), causing eye inflammation and corneal abrasions, and xerostomia (dry mouth) which leads to oral candidiasis, caries, and other oral infections [2]. Even though the etiology and pathogenesis are not fully known, studies have shown that Sjögren's syndrome might be the result of various factors that include genetic predisposition, environmental factors, hormones, and immune dysregulation [3]. Sjögren's syndrome patients have also been diagnosed in conjunction with other autoimmune diseases, such as rheumatoid arthritis, systemic lupus erythematosus (SLE), and systemic scleroderma [4–7].

Even though the pathogenesis of pSS is not entirely comprehended, it has been shown that it can be a result of both innate and adaptive immune response; an increase in CD4 T cells induces inflammatory cytokines, which is directly related to the augmented secretion of B cells, a key feature of primary Sjögren's syndrome, resulting in high secretion of autoantibodies, that precedes most autoimmune diseases [4,8]. More than 60% of patients suffering from pSS show irregular levels mostly of autoantibodies such as anti- SS-A/Ro or anti SS-B/La, muscarinic receptor, anti-fodrin receptor antibodies, and rheumatoid factor, causing aggravating symptoms and life-threatening comorbidities. While these specific antibodies might not be specific for this autoimmune disease, it has been shown that they are associated with the early development of the disease, also they might be responsible for salivary gland lymphocytic infiltration and dysfunction, hypergammaglobulinemia and other dysfunctions related to high B-cell activation [9].

Metformin is a well-known prescription drug for Type II diabetes, an oral anti-hyperglycemic agent that improves insulin sensitivity via AMPK-dependent and AMPK-independent mechanisms, resulting in a direct decrease in glucose. Metformin has also been studied for its anticancer effects exhibiting a decrease in regulatory T cells in tumors, and inhibitory effects on angiogenesis [10]. In a recent study, metformin was discovered as a newfound benefit in autoimmune diseases, for showing anti-inflammatory antiproliferative, antifibrotic, antioxidant effects and immunomodulatory effects [5–7]. Other studies have also suggested that metformin actions go further, such as germinal center formation, macrophage polarization, cytokine production, etc, thereby

* Corresponding author.
E-mail address: singhbb@uthscsa.edu (B.B. Singh).

https://doi.org/10.1016/j.jtauto.2023.100210
Received 7 June 2023; Received in revised form 14 August 2023; Accepted 29 August 2023

Abbreviations

(pSS)	Primary Sjogren's syndrome
(*Ca2+*)	calcium
(IL14α)	*Interleukin 14 α*
(*ER*)	Endoplasmic reticulum
(DAMPS)	Danger-Associated Molecular Patterns

making metformin a candidate for treatment for immune-mediated diseases [11]. Similarly, metformin has been shown to reduce salivary gland inflammation and decreased in pSS incidences were observed in patients taking metformin [12,13], suggesting that it can help Sjögren's patients, but the mechanism is not known.

B cell growth factor cytokine IL-14α was first identified from Burkitt lymphoma cells, and it was associated with increased B cell proliferation, mainly of germinal center B cells that includes B1 cells (CD5 positive) and activated B2 cells (CD5 negative). Importantly, B1 population have been further divided into two subpopulations: B1a lymphocytes that express CD5, and B1b lymphocytes that do not express CD5, but share all the other attributes of B1 cells [14], thus could be further used to differentiate various B cells in SS patients. It was well established that transgenic mice IL-14α exhibits a phenotype that is very similar to some autoimmune diseases, such as Systemic lupus erythematosus (SLE) and Sjögren's syndrome [15]. These transgenic mice expressing IL-14α in the B cell compartment has demonstrated first an increased autoantibodies and cytokines, followed by hypergammaglobulinemia, lymphocytic infiltration of parotid glands and large B cell lymphomas, all symptoms observed in SS patients [15–18]. Thus, we use IL-14α Tg mice as a model for Sjögren's syndrome progression and showed that metformin treatment decreases lymphocytic infiltration, restore saliva production, and blocks DAMPS (danger-associated molecular patterns) release. Moreover, to understand the mechanism, we showed that metformin treatment also inhibits ER stress progression on IL-14α Tg mice and increase Ca^{2+} signaling.

2. Materials and methods

2.1. Human samples, animals, and HSG cells culture

8-12 female mice all 9-month-old of age, control (wild type; C57BL/6) and IL14α Tg were used for these experiments. The IL14α Tg-mice were generated as previously described in Refs. [15,16]. Animals were housed in an AAALAC accredited animal housing close monitored by the University of Texas-San Antonio Laboratory Animal Resources where temperature is controlled under a 12/12-h light/dark cycle with free access to food and water. Institutional guidelines were followed in all animal experiments. To study the effect of metformin (Sigma, St. Louis, MO) on IL14α Tg-mice, animals were fed orally using polypropylene feeding tubes (Instech, Plymouth Meeting, PA USA). The compound was given daily for 90 days at the concentration of 5 mg/kg bodyweight/day. Once the treatment timeline was ended mice were sacrificed and organs and blood collected for experiments. Human minor salivary glands that fulfilled the 2016 ACR-EULAR criteria for pSS were classified as pSS whereas patients that do not show at least 4 classifications (lymphocytic sialadenitis with a focus score $\geq$1 foci/mm^2, autoantibodies positivity, Schirmer test $\leq$5 mm/5 min, and an unstimulated salivary flow rate $\leq$0.1 ml/min) were identified as non-SS (nonSS-SICCA) and were used as controls from NIH. Informed consent was obtained from patients and the samples used were discarded tissues without identifying information after disease diagnosis. Human Submandibular Gland (HSG) cells [19] were cultured (2×10^6 cells/ml) in MEM medium supplemented with 10% FBS, penicillin (50U/ml) and streptomycin (50 μg/ml) and cells were maintained at 37 °C with 95% humidified air and 5% CO_2.

2.2. Saliva collection and analysis

All C57BL/6 wild type and IL14α Tg mice were anesthetized 5 min before testing and then intraperitoneally injected with pilocarpine (0.5 mg/ml) at 1 μl/g body weight (Sigma, St. Louis, MO). Following the injection, mice were laid on heated (37 °C) small blue hospital pads (Size 23 × 36 inch) with the head tilted slightly downward into a pre-weighted 1.0 ml tube (Eppendorf, Enfield, CT) the secreted saliva was collected in every 4 min interval for a total length of 16 min and was quantified gravimetrically.

2.3. Immunohistochemistry and imaging

C57BL/6 wild type and IL14α Tg (n = 8) mice had their salivary glands removed and fixed in 4% paraformaldehyde for up to 5hr then transfer to a 70% ethanol container and sent to University of Texas-San Antonio Histology and Immunohistochemistry Laboratory. Paraffin-embedded, formalin-fixed human and mice salivary gland tissue sections, 5-μm-thick, were stained with hematoxylin and eosin (H&E) and focal lymphocytic infiltration areas in H&E slides were captured and assessed using BZ-X800 All-in-one Fluorescence Microscope technology (Keyence, Osaka, Japan). For fluorescent confocal imaging, salivary gland sections from respective animals were permeabilized with 0.1% TritonX-100 in PBS (pH 7.4), blocked (using 5% BSA in PBS) and probed overnight with the respective primary antibodies in a hydrated chamber maintained at 4 °C. Following incubation with the primary antibodies, the slides were washed and incubated with fluorophore-conjugated respective secondary antibodies for 1 h at room temperature. Thereafter the slides were washed, and coverslip mounted using Vectashield hardest mounting media with DAPI (Vector Laboratories, CA). Images were acquired at 10x magnifications using a confocal laser LAS X Life Science Microscope (Leica Microsystem, Deerfield, IL). Morphological details and fluorescence were analyzed using Image-J software (NIH). The microscopic images were imported to Keyence BZ-X800 analyzer (Osaka, Japan), selected areas (n = 4) at low magnification were used for infiltration analysis into the salivary gland tissue, once confirmed at high magnification that invasive proliferation of cells was present. To count the infiltrated cells, we use the function Hybrid cell counter at higher magnification.

2.4. $[Ca^{2+}]i$ measurements

Fura2-AM fluorescence in single cells was measured by microfluorimetry using a TILL Photonics spectrofluorimeter (Polychrome 4, Applied Scientific Instrumentation and TILL Photonics In., Eugene, OR) attached to an inverted Olympus X70 microscope with a Fluor 40x oil-immersion objective. Images were acquired using an enhanced CCD camera and the Metafluor software (Universal Imaging Corporation, PA).

2.5. Electrophysiology

For patch clamp experiments, coverslips with cells were transferred to the recording chamber and perfused with an external Ringer's solution of the following composition (mM): NaCl, 145; KCl, 5; MgCl2, 1; CaCl2, 1; Hepes, 10; Glucose, 10; pH 7.4 (NaOH). Whole cell currents were recorded using an Axopatch 200B (Axon Instruments, Inc.). The patch pipette had resistances between 3 and 5 M after filling with the standard intracellular solution that contained the following (mM): cesium methane sulfonate, 150; NaCl, 8; Hepes, 10; EGTA, 10; pH 7.2 (CsOH). Basal leaks were subtracted from the final currents and average currents are shown. The maximum peak currents were calculated at a holding potential of −80 mV. The I–V curves were made using a ramp protocol ranging from −100mV to +100 mV and 100 ms duration was delivered at 2s intervals, whereby current density was evaluated at various membrane potentials and plotted. All experiments were carried

out under room temperature.

2.6. Flow cytometry

For cell markers staining, cells were obtained from submaxillary glands and blood from all mice. First, to isolate the cells from the tissue, submaxillary glands were cut into pieces of 2–3 mm and incubated in 1 mg/ml sterile collagenase solution (Roche Diagnostics, Mannheim, Germany) in PBS (Corning, Corning, NY) for 1 h at 37 °C, once digestion was completed, the cell suspension was filtered through a 70-μm nylon Falcon cell strainer (Becton Dickinson, San Jose, CA), and resuspended in FACS buffer (1% BSA and 0.05% sodium azide in PBS) at a concentration of 2×10^6 cells/ml. Second, whole blood was collected by cardiopuncture protocol [20], and peripheral blood mononuclear cell (PBMC) isolation were performed by density gradient centrifugation using Histopaque®-1077 (Sigma, St. Louis, MO) solution, separated cells were washed with PBS (Corning, Corning, NY) twice, resuspended in Flow cytometry buffer before staining, and run through BD LSRII flow cytometer, where 10,000–20,000 events were acquired per sample, data was analyzed using FlowJo 9.0 (San Jose, CA, USA). Various combinations of antibodies labeled with fluorescent-labeled anti-mouse antibodies anti-were used at dilutions indicated below.

List of antibodies.

Antibody	Host	Clonality	Dilution factor	Company
CD8α (2.43)	Rat	Monoclonal	1:50	Cell Signaling
CD3 (17A2)	Rabbit	Monoclonal	1:1600	Cell Signaling
ELF-2α (D7D3)	Rabbit	Monoclonal	1:1000	Cell Signaling
NK1.1	Mouse	Monoclonal	1:200	Abcam
CD11c (D3V1E)	Rabbit	Monoclonal	1:200	Cell Signaling
CD8α (D4W2Z)	Rabbit	Monoclonal	1:1000	Cell Signaling
CD19 (eBio1D3 (1D3))	Rabbit	Monoclonal	1:1000	ThermoFisher
CD4 (GK1.5)	Rabbit	Monoclonal	1:1000	ThermoFisher
CD194 (CCR4) (D8SEE)	Rabbit	Monoclonal	1:1000	ThermoFisher
CD11b (M1/70)	Rabbit	Monoclonal	1:1000	ThermoFisher
CD49b (HMA2)	Rabbit	Monoclonal	1:1000	ThermoFisher
CD183 (CXCR3)	Rabbit	Monoclonal	1:1000	ThermoFisher
CD196 (CCR6)	Rabbit	Polyclonal	1:1000	ThermoFisher

2.7. Measurement of alarmins and cytokines levels

HGMB1, Histone 3, hsp70 levels in the supernatant were measured using the Enzyme-Linked ImmunoSorbent Assay (ELISA) kit (Life Technologies, Carlsbad, CA, USA) following the manufacturer's instructions using standard diluent buffers designed for use with mouse supernatant. All samples were measured on a single 96-well plate for each cytokine, the cultured medium was centrifuged at 800 G at for 5 min 4 °C and the supernatant was used as the sample. Based on that criterion, all cytokine values for the HSG supernatant samples examined were above the limit of detection and within the reportable range of each assay.

2.8. Statistical analysis

Data analysis was performed using Origin 9.0 (OriginLab, Northampton, MA) and Graphpad prism 8.0 (San Diego, CA). Statistical comparisons were made using Student's *t*-test. Experimental values are expressed as means ± S. D or means ± S.E. Differences in the mean values were considered to be significant at $p < 0.05$.

3. Results

3.1. Lymphocytic infiltration in salivary glands is observed in Sjögren's syndrome

It has been established that primary Sjogren's syndrome (pSS) patients present histopathologic presence of lymphocytic infiltration of the salivary and other exocrines glands of the respiratory tract. Studies showed that the infiltrate is comprised by B and T cells mostly, with the predominance of CD4 T^+ cells, characterizing by a chronic inflammation and gland degradation [21,22]. To initially conform and to obtain a deeper understanding of the lymphocytic infiltration on pSS patients against control, we obtained images of a salivary gland tissue stained with hematoxylin and eosin (H&E) protocol showing increased lymphocytic infiltration displayed in pSS patients (data not shown). To identify what type of lymphocytes were preset in the samples, we performed immunofluorescence staining to detect immune cells revealing an increased number of B cells, monocytes, and natural killer (NK) cells in pSS samples (Fig. 1A). These results are consistent with studies showing that shows that pSS patients are known to display B-cell hyperactivity and increased inflammatory levels. Activated T cell-mediated B cell activation is a marker of pSS progression; thus, we also investigate the characteristics of the T cell infiltration. Importantly, we use microscopic immunohistochemistry for the expression of CD3, a known marker for T cells along with ELF-3 a transcription factor, that is critical for T cell activation in pSS samples against control. pSS samples displayed a higher expression of $CD3^+ELF\text{-}3^+$ when compared with control patient samples (Fig. 1B). Overall, the H&E and immunohistochemistry staining showed that pSS demonstrated a high level of lymphocytic infiltration in salivary glands characterized mainly by B and T cells.

In comparison with our human data, we use 6-month-old IL14α Tg mice, a known mice model for Sjogren syndrome, and observed an increase in lymphocytic infiltration (Fig. 1C). We next characterized the different types of lymphocytes were present between age- and gender matched wild types and IL14α Tg 6-month-old mice by flow cytometry. Our data shows that there is a significant increase of B cells, monocytes, and T cells in IL14α Tg mice than its counterpart wild type (Fig. 1D). For a better understanding of when the progression of the disease occurs in mice, we performed flow cytometry in PBMCs (peripheral blood mononuclear cells) from these mice at different ages (1, 6 and 12 months old). We use markers for B cell (CD19 APC), monocytes (CD11b FITC), $CD4^+$T cell (PE), $CD8^+$T cell (eFlour450), $Th1^+$ ($CXCR3^+$ PerCP-cy5.5) and $Th17^+$ (NK 1.1 PE-Cy7). We observed an increase of lymphocytes starting at 6-month-old along with B and T cells (Fig. 1E). Together these results are consisted with studies showing that lymphocytic infiltration is a main trait on the progression of the pathogenesis of Sjögren's syndrome, and its largely comprised by an increase of B cells, that in turns promotes inflammation [23–25].

3.2. Lymphocytic infiltration in salivary gland tissue in IL14α Tg mice is reversed by metformin treatment

As current therapies have limited success in pSS patients, we started evaluating with FDA-approved drugs to see if they can reverse Sjogren's Syndrome symptoms in mice. Studies have shown that metformin can be used as a treatment for different autoimmune diseases, due to its immunoregulation ability to decrease inflammation [13]. To further investigate the effects of Metformin on the progression of Sjogren's syndrome, we gathered 16 IL-14α Tg 6-month-old female mice and divided them into 2 groups, one was the control group where we fed them saline in a daily basis, the treatment group was fed metformin orally daily at a concentration of 5 mg/kg of body weight. On day 0, all mice were weighted and randomly distributed into two groups; after that on day 1 we started the treatment, after 90 days animals were sacrificed and blood, saliva, and salivary gland were collected for

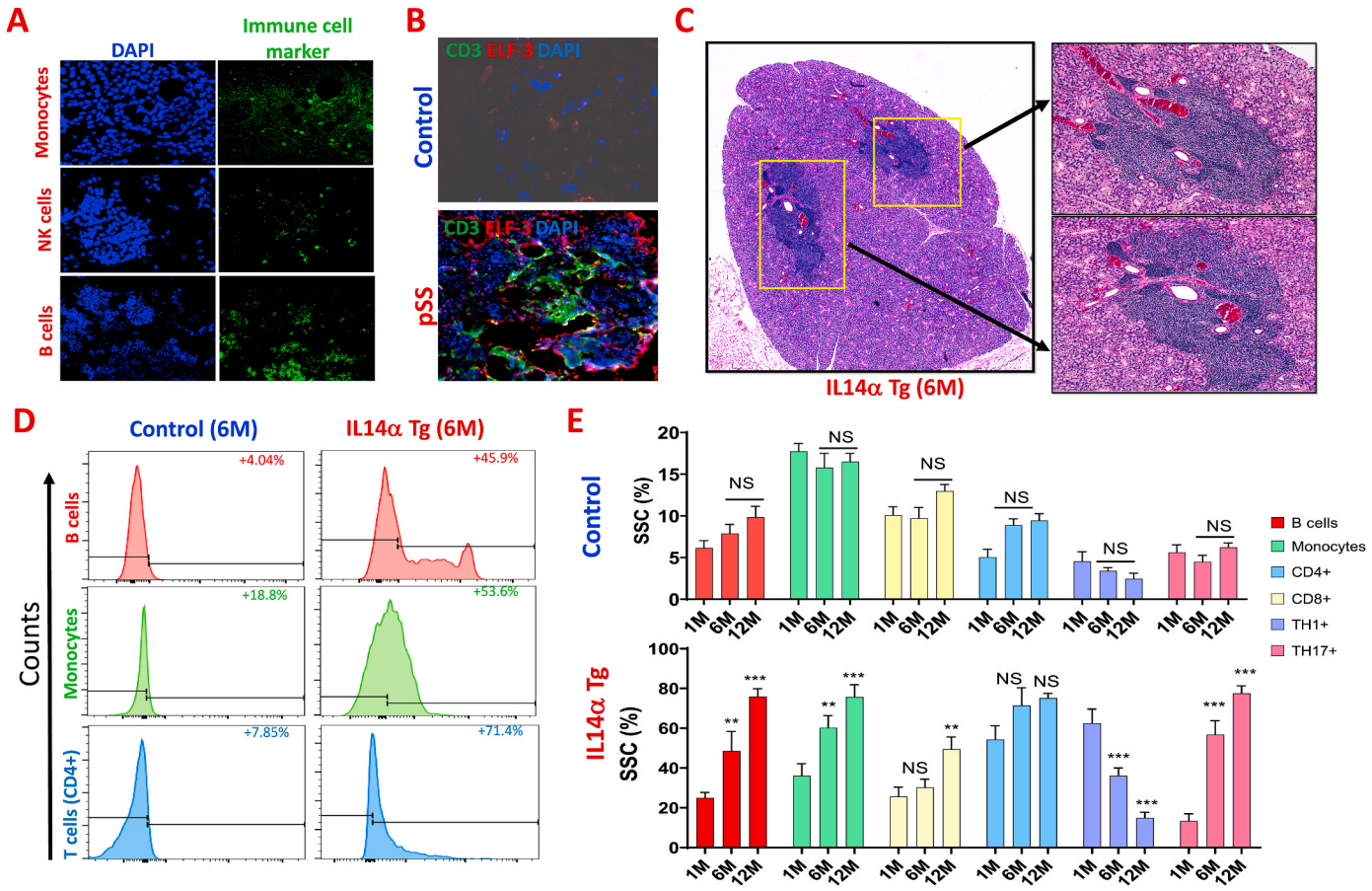

Fig. 1. *Primary* SS patients and IL14α-mice shows immune cell infiltration. Patients showing immune characteristics and IL14α Tg mice (n = 8) salivary glands were analyzed for immune cell infiltrations. (A) Confocal images showing the expression of immune cells on the pSS slides and the activation of ER stress. Samples were first stained with CD14 (monocyte cell marker) (FITC), CD19 (B cell marker) (FITC) and NK1.1 (Natural killer cell marker) (FITC) in salivary glands from primary Sjogren's syndrome (pSS) samples, representing immune cell infiltration in selected tissue. (B) Subsequently, analogous samples were stained with CD3 and ELF-2α showing the increased ER stress in infiltrating lymphocytes in SS patients' salivary glands against control patients. The images shown are representations of three individual experiments. (C) Shows H&E staining in salivary gland of 6-month-old IL14α Tg-mice showing immune cells infiltration (images are representation of 6 individual samples performed in triplicate). On the smaller pictures we show the augmented presence of infiltrated immune cells. (D) Lymphocytes were isolated from salivary glands of 6-month-old IL14α mice (n = 8) and control littermates (n = 8). Afterwards cells were stained with anti-CD19 (PerCP-Cy5.5), anti-CD4 (PE), and anti-CD11b (APC) using multi-color flow cytometry. (E) Bars represent the immune cells quantification from flow cytometry, isolated from salivary glands from IL14α Tg and control mice from different ages (1, 6 and 12 months), cells were stained with anti-CD11b (marker for monocytes), anti-CD4 and anti-CD8 (marker for T cells), anti-CD19 (marker for B cells), anti-CXCR3 (marker for Th1 T cells) and anti-CCR6 (marker for Th17 T cells). Age groups used are indicated in the figure and the images shown are representation of 3 separate experiments. Data shown are representative of three independent experiments with similar results. Bar graphs depict average ± SD for relative values, ***p ≤ 0.001, **p ≤ 0.01, NS = non-significant (Student's *t*-test).

experiments (Fig. 2A). First, in order to determine if metformin treatment would influence salivary gland function, we next evaluated saliva secretion in saline and metformin treated IL-14α Tg mice. Saliva secretion was initiated by the addition of pilocarpine, and both total saliva and the flow between the two groups were evaluated. Interestingly, there was a significant increase in the total saliva secretion in metformin treated IL14α Tg-mice when compared with saline-treated IL14α Tg mice (Fig. 2B). Similarly, an increase in flow rate was also observed in IL14α Tg-mice that were treated with metformin (Fig. 2C). Collectively these results showed that metformin treatment can recover salivary gland dysfunction in IL14α Tg mice, which is a major condition in the progression of SS disease.

To further evaluate the effect of metformin in reversing immune cell infiltration, we initially quantified the infiltration of lymphocytes in salivary gland tissue. Studies have shown that metformin is a key component for cancer and autoimmune diseases, due to its antitumor activity and immunomodulatory effects, besides its use for diabetes treatment [26]. Microscopic images of H&E-stained slides were analyzed from IL14α Tg-mice treated with metformin daily (orally 5 mg/kg of body weight) and with saline (control), we show that a significant decrease of immune cell infiltration is observed in the metformin-treated IL14α Tg-mice in comparison with control saline treated IL14α Tg-mice (Fig. 2D and E), which showed multiple foci formation in the salivary gland tissue (Fig. 2D). Quantification of the immune cell infiltration was also determined, which confirmed that the number of infiltration (calculation obtained by counting nuclei formation on specific and pre-determined areas on both groups) was significantly decreased in metformin treated IL14α Tg-mice (Fig. 2F). Furthermore, we also determined the impact of metformin treatment on the immune cells that were infiltrated in the salivary gland tissue. After collecting the salivary gland, tissue was washed in PBS (1x) then cell disintegration was performed before staining the cells with immune cell markers. Cells were stained with markers for B cells (CD19 APC), monocytes (CD11b FITC), macrophages F4/80 (Alexa Fluor 594), $CD4^{+}$T cell (PE), dendritic cells (MHC II APC-Cy7) and natural killers (CD49b PE-Cy7) (Fig. 2G). Importantly, we observed a significant decrease in all tested immune cells obtained from tissue lysates from animals treated with metformin and control, suggesting that this drug is vital for the weakening of the progression of this disease.

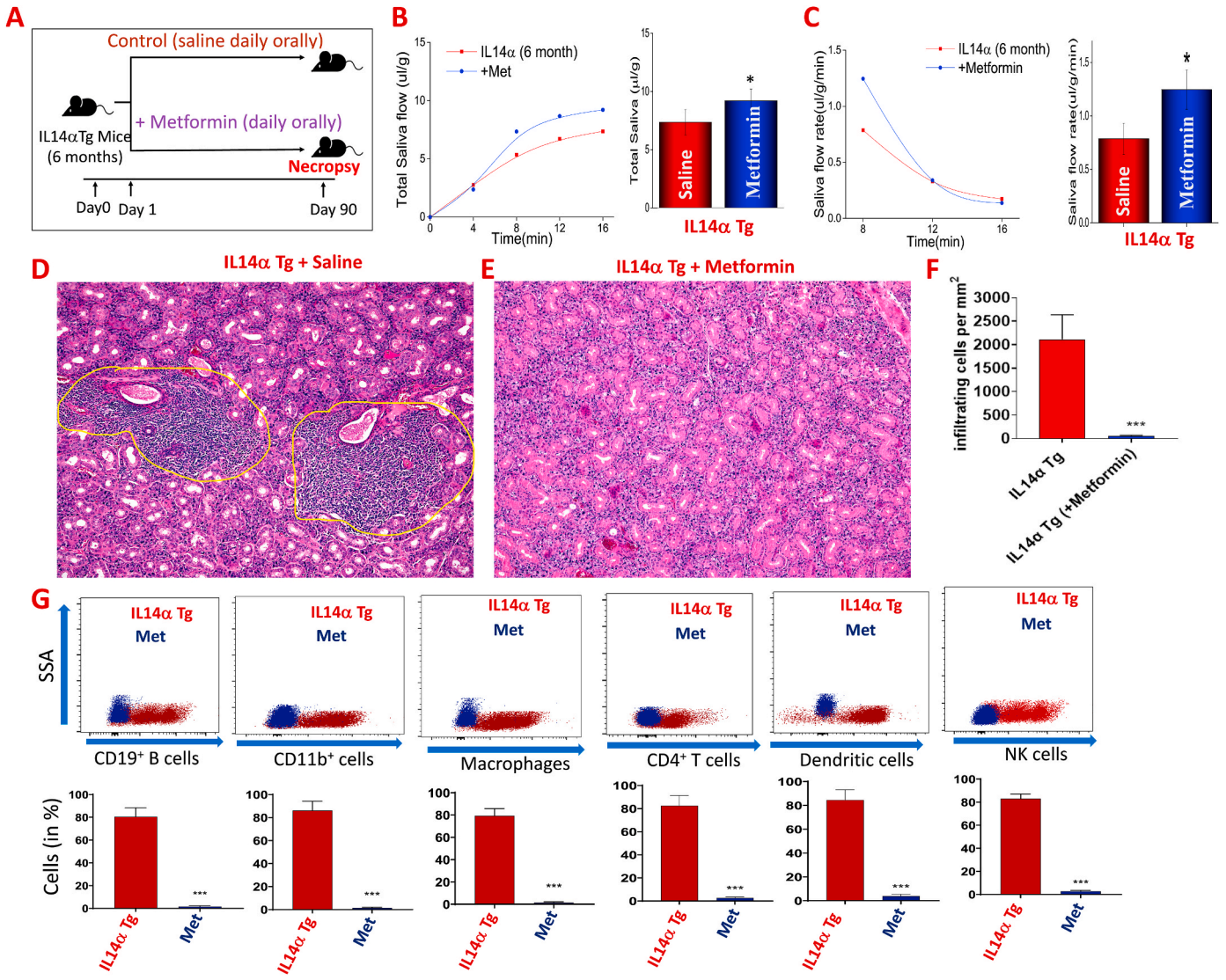

Fig. 2. Decreased in immune cells infiltration observed in IL14α Tg-mice when treated with Metformin: Metformin treatment improves IL14α Tg mice inflammatory levels. (A) Schematic illustration showing 6 months old IL14α Tg mice were treated with metformin (n = 8) or saline (control, n = 8) for 90 days and then sacrificed. Salivary glands, blood and saliva were used for further analysis. (B) Saliva flow rate in 6-month-old IL14α Tg mice treated with Metformin and saline alone is shown as line graph, which showed a time-dependent decrease in saliva secretion. Quantification of saliva flow is shown as bar graph. Error bars represent means ± SE. * indicates $p \leq 0.05$ difference between the two groups. (C) Saliva secretion was induced by pilocarpine in 6-month-old IL14α Tg mice treated with Metformin and saline alone and plotted. The data presented are representative of 6–8 animals in each group. Saliva was collected every 4 min, and total saliva secreted is plotted as line graph. Quantification of total saliva secreted is shown as bar graph. Error bars represent means ± SE. * indicates $p \leq 0.05$ difference between the two groups. (D–E) Shows H&E staining in salivary glands from 6-month-old IL14α Tg-mice with saline and treated with metformin for 90 days, the presence of immune cells is singled out (images are representation of 3 individual samples performed in duplicate). (F) Bar graph showing percentage of infiltration cells from the tissue samples from Fig. 1D and E. Images shown are representation of 3 individual experiments. Values are expressed as mean ± SE. *** indicates significance $p < 0.001$. (G) Lymphocytes were isolated from salivary glands of 6 months old IL14α mice treated with saline and metformin (for 90 days). Flow cytometry was performed, and the isolated cells were stained with anti-CD19 (PerCP-Cy5.5), anti-CD11b (PE), anti-F4/80 (Pacific blue) anti-CD4 (PE-Cy7), anti-MHCII (FITC), and anti-CD49b (Alexa-Fluor 647) using multi-color flow cytometry. Bar graphs represent the percentage of total number cells marked positively for the specific markers. Data shown are representative of three independent experiments with similar results. Bar graphs depict average ± SD for relative values, ***$p \leq 0.001$ (Student's *t*-test).

3.3. Ca^{2+} signaling is restored in HSG cells by metformin treatment

To further establish the mechanism as how metformin can reverse a complex part of SS pathology, we evaluated the effects of metformin treatments in key signaling processes. Ca^{2+} signaling is not only critical for saliva secretion, but also maintains immune cell function [27–29]. Importantly, primary acinar cells isolated from IL14α Tg-mice showed a difference in Ca^{2+} signaling. Addition of thapsigargin (Tg, 2 µM in the absence of extracellular Ca^{2+}), which is a potent blocker of the sarcoendoplasmic reticulum Ca^{2+} transport ATPase and depletes intracellular Ca^{2+} stores, showed a significant increase in cytosolic Ca^{2+} levels (first peak) in primary salivary cells obtained from submandibular glands of control saline and metformin-treated IL14α Tg-mice (Fig. 3A). Importantly, ER Ca^{2+} levels were significantly higher in acinar cells obtained from metformin-treated IL14α Tg-mice (Fig. 3A and B). Similarly, Tg-stimulated Ca^{2+} entry (second peak) was also significantly higher in acinar cells obtained from metformin-treated IL14α Tg-mice (Fig. 3A and B). Next, we evaluated if metformin effect is dose dependent and a gradual increase in intracellular Ca^{2+} levels ($[Ca^{2+}]_i$) was observed upon the addition of metformin (Fig. 3C–G). Our previous studies have identified that TRPC1 is important for Ca^{2+} entry in salivary gland cells that modulates saliva secretion [30,31]. To further

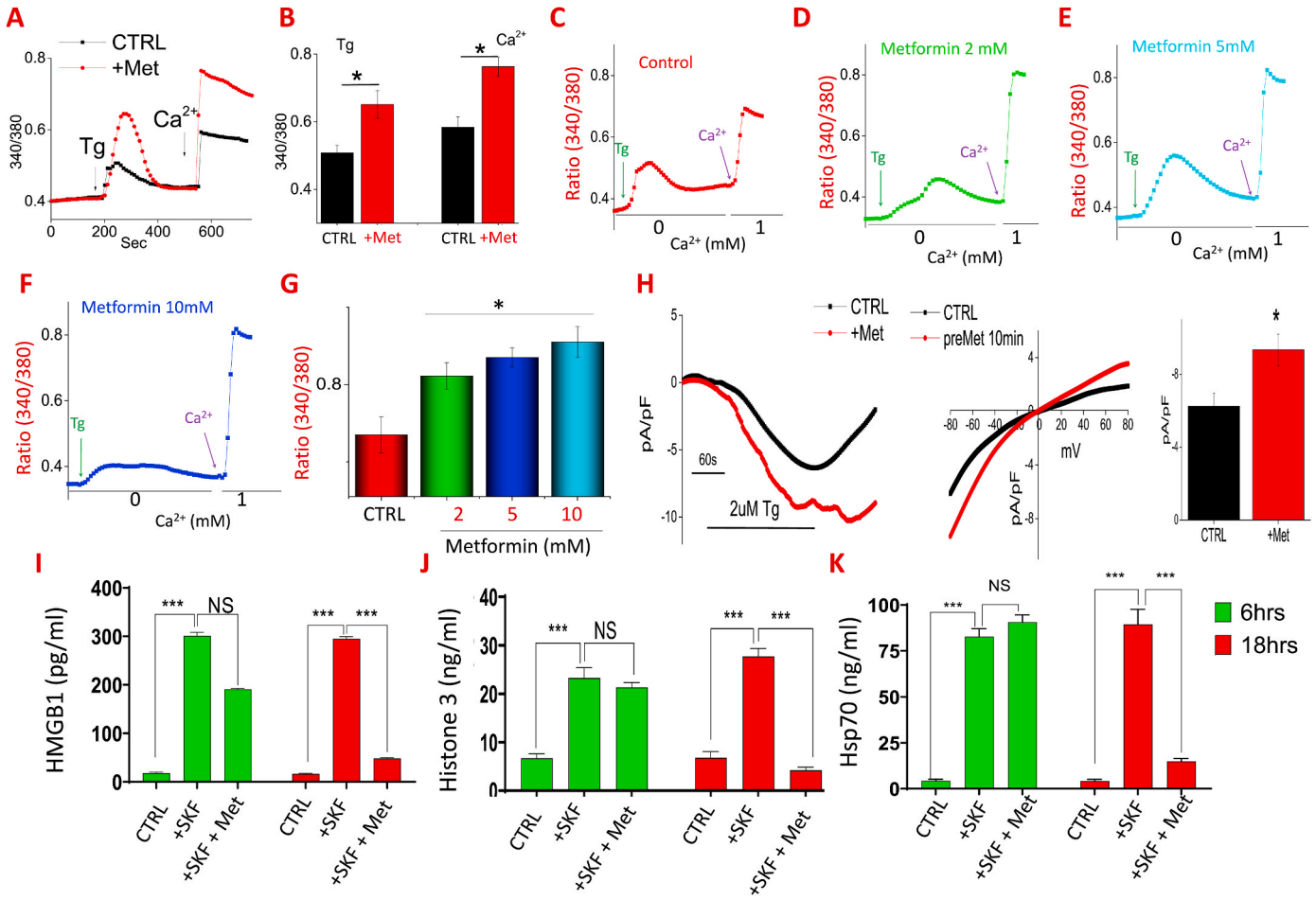

Fig. 3. Ca^{2+} signaling recovery in IL14α Tg-mice after metformin treatment. (A) Representative traces in acinar cells showing Tg-mediated ER calcium release and calcium entry in control and metformin treated IL14α Tg mice. Quantification of the ER calcium release and calcium entry is shown as bar graph from 100 to 150 individual acini's is shown in (B). *p ≤ 0.05, (Student's *t*-test). (C–F) Representative calcium traces in human submandibular gland cells showing Tg-mediated calcium entry in various metformin concentrations (0–10 mM) added 10 min prior to the addition of thapsigargin. (H), shows representative Tg-induced currents in controls and metformin (10 mM) treated cells. IV curves as well as quantification of the current intensity is shown as bar graph. *p ≤ 0.05, (Student's *t*-test). (I–K) Damage-associated molecular patterns (DAMPs) were analyzed, by colorimetric analysis in supernatants of HSG cells after SKF96365 (10 μM) and Metformin (5 mM) treatment for 6hrs and 18hrs. Data shown are representative of three independent experiments with similar results. Bar graphs depict average ± SD for relative values, ***p ≤ 0.001, NS = non-significant (Student's *t*-test).

establish that increase in Ca^{2+} entry is observed in metformin-treated IL14α Tg-mice, whole-cell current recordings were performed in submandibular cells. Addition of thapsigargin (store depletion) induces an inward current which was non-selective in nature and reversed at 0 mV (Fig. 3H). Importantly, the channel properties were similar as those previously observed with TRPC1 channels and metformin-treatment showed a gradual increase in Ca^{2+} entry (Fig. 3H). data presented thus far suggest that metformin increases Ca^{2+} entry that was critical for the inhibition of salivary gland dysfunction and/or immune cell infiltration.

To further elaborate on possible mechanisms, we evaluated danger-associated molecular patterns (DAMPs) release in control saline or metformin-treated IL14α Tg-mice. It's been established that DAMPS play a key role in the pathogenesis and progression, we use human submandibular gland (HSG) cell line to observe the effects of metformin with ER stress inducers or calcium channel blockers such as SKF-96365, Tunicamycin and BFA in the release of HMGB1, Histone 3 and Hsp70, it is well established that ER stress is characterized by release of DAMPs into the blood stream which results in persistent inflammation, leading to chronic diseases [32]. We seeded HSG cells (2×10^6 cells/ml) and treated them with SKF-96365 (10 μM) for 6hrs and 18hrs (Fig. 3I–K) and we evaluated the levels of released DAPMS in the media by ELISA assays. Interestingly, the levels of histone-3, HMGB1 and hsp70 in the cells treated with metformin in the presence of SKF-96365 were significantly decreased when compared with cells treated with SKF-96365 alone. These results show that the power of the treatment with metformin can be extended to also block calcium channels blockers mechanisms [33]. To further substantiate our results, we repeated the same assay with Tunicamycin and BFA (Fig. 1SA-C) and obtained similar results.

3.4. *ER stress markers are decreased in IL14α Tg mice treated with metformin*

Data presented in this study up to now, confirmed that metformin treatment demonstrated the ability to reverse *in vitro* SS symptoms. Our next step was to see if the treatment would affect the activation of ER stress markers, a key characteristic seen in old IL14α Tg mice. CHOP (C/EBP homologous protein) and GRP78, also known as BiP, are key regulators for endoplasmic reticulum (ER) stress due to their role as ER chaperones which control the activation of ER stress sensors, such as IREIα (inositol-requiring enzyme 1α) and ATF6 (activating transcription factor 6), transmembrane receptors known to activate the unfolded protein response (UPR) [31,34]. We assessed the expression of these ER stress markers in salivary gland tissue in metformin treated IL14αTg

mice (n = 8) against control animals (n = 8). Representative microscopic images show a significant reduction in the presence of ER stress marker expression in treated tissue against control (saline treatment) ones (Fig. 4A–D). In aggregate, these findings demonstrate that metformin inhibits the activation of ER stress by restoring Ca^{2+} signaling, preventing further damage to the tissue.

4. Discussion

Sjögren's syndrome (pSS) is a systemic autoimmune disease that mainly affects the exocrine glands, mostly salivary and lacrimal glands. Patients may experience dry eyes, causing a gritty or burning sensation, and dry mouth, leading to difficulty in swallowing, speaking, and an increased risk of oral/dental problems [21,35]. pSS is also associated with lymphocytic infiltration in the affected glands, mainly composed of B cells and T cells ($CD4^+$) that mistakenly target and attacks the exocrine glands, leading to inflammation and damage. Although lymphocytic infiltration is observed, currently available immunotherapies have limited success in pSS patients, suggesting that additional factors or mechanism might be critical. Thus, in this study using primary Sjogren's syndrome (pSS) patients and IL14α Tg mice, we provide valuable insights into the disease process, and establishing the potential therapeutic effects of metformin in reversing the disease progression.

The histopathological analysis of salivary gland tissue from pSS patients confirmed the presence of lymphocytic infiltration. This observation is consistent with previous studies highlighting the chronic inflammation and gland degradation associated with pSS. Immunofluorescence staining further revealed an increased number of B cells, monocytes, and natural killer (NK) cells in pSS samples, indicating B-cell hyperactivity and increased inflammatory levels, which are characteristic of the disease [36,37]. Importantly, the IL14α Tg mouse model, which mimics Sjogren's syndrome, was further used to investigate the lymphocytic infiltration in mice. Flow cytometry analysis demonstrated a significant increase in B cells, monocytes, NK cells, and T cells in IL14α Tg mice compared to wild-type mice. These findings align with previous studies suggesting that lymphocytic infiltration plays a crucial role in the pathogenesis of Sjogren's syndrome [38,39].

To explore potential therapeutic options, this study evaluated the effects of metformin, an FDA-approved drug with immunoregulatory properties, in IL14α Tg mice. Treatment with metformin led to a recovery of salivary gland function, as indicated by increased saliva secretion and flow rate. Moreover, metformin administration resulted in a significant reduction in immune cell infiltration in salivary gland tissue, supporting its potential as a treatment option for Sjogren's syndrome. To further identify the mechanism, our data revealed that metformin has the ability to restore Ca^{2+} signaling in primary acinar cells isolated from IL14α Tg mice. Metformin treatment showed a dose-dependent increase in intracellular Ca^{2+} levels, which was mediated through TRPC1 channels (a non-selective currents was observed, and the current properties mimicked as observed with TRPC1 [40,41]. Importantly, TRPC1 has been previously shown to modulate saliva secretion [42,43]. This suggests that metformin's impact on TRPC1-mediated Ca^{2+} signaling contributes to the inhibition of salivary gland dysfunction and immune cell infiltration.

To further understand the consequences of the loss of calcium signaling, our data showed that IL14α Tg mice had an increase in ER stress markers, which were decreased upon metformin treatment. The expression of CHOP and GRP78, key regulators of ER stress, was significantly reduced in salivary gland tissue from metformin-treated mice compared to control animals. This suggests that metformin inhibits the activation of ER stress by restoring Ca^{2+} signaling, thereby preventing further damage to the tissue. Along with ER stress, danger-associated molecular patterns (DAMPs) could play a critical role in the pathogenesis and progression of Sjogren's syndrome. Metformin treatment further showed a decrease in the release of DAMPs, such as HMGB1, Histone 3, and Hsp70, in salivary cells, indicating its potential as an effective treatment in preventing persistent inflammation associated with ER stress [33,44].

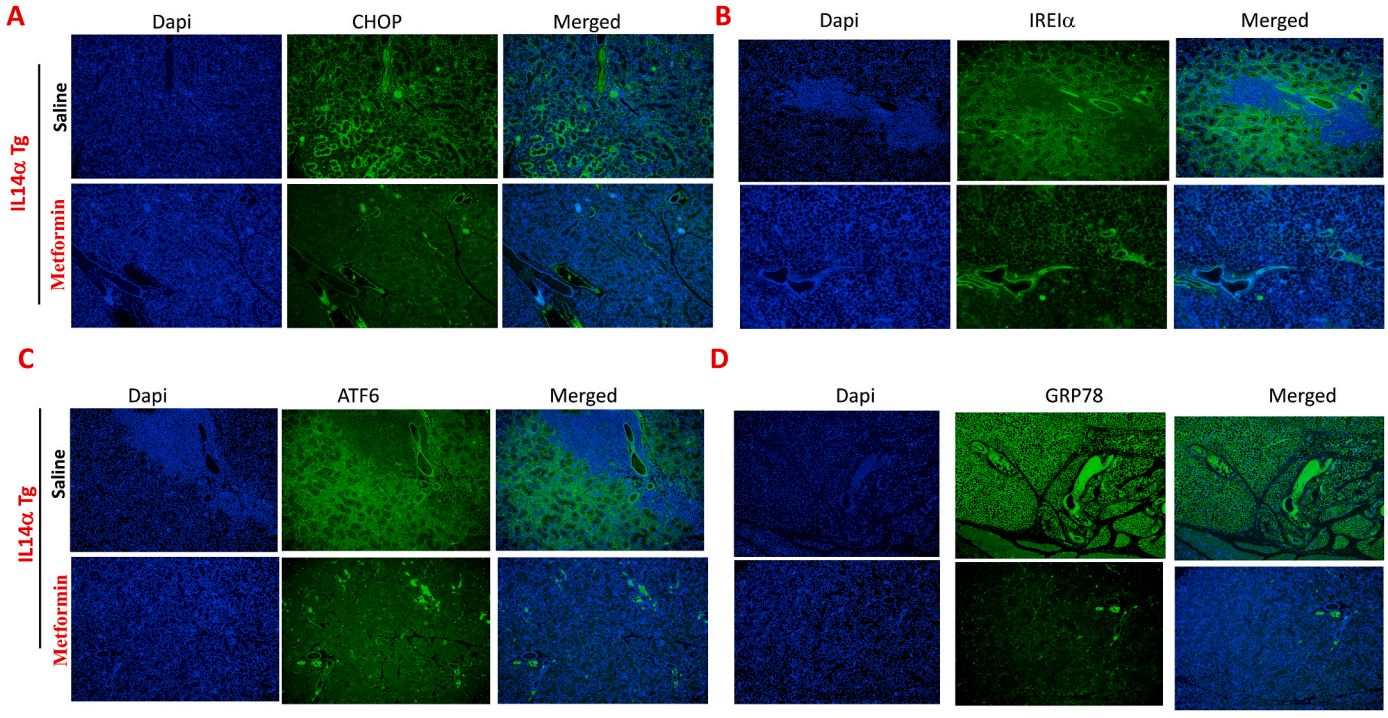

Fig. 4. ER stress levels in tissue samples of salivary glands of IL14α mice are reduced by Metformin treatment. (A–D) Confocal images showing the expression of ER stress markers (CHOP, IREIα, ATF6 and GRP78) in salivary glands from 6-month-old IL14α mice treated with saline and metformin for 90 days. Samples were stained with Alexa-Fluor 488 labeled secondary antibodies (green) and nuclei were counterstained with DAPI (blue). Results were viewed in fluorescence microscopy; the scale bar represents 20 μm. Images shown are representation of 3 individual experiments.

Overall, the findings of this study highlight the significance of lymphocytic infiltration in the pathogenesis of Sjogren's syndrome and provide evidence for the potential therapeutic effects of metformin in reversing the disease progression. The restoration of salivary gland function, due to the modulation of Ca^{2+} signaling that prevents ER stress and the release of DAMPs, could be the key in the reduction in immune cell infiltration, thereby indicating the promising role of metformin as a treatment option for Sjogren's syndrome. However, further studies are warranted to translate these findings into clinical applications for the benefit of pSS patients.

Credit author statement

Author Contributions: Conceptualization, methodology, designing research studies, reagents, and data analysis, V.N.D.C., Y.S., J A., B.B.M., and B.B.S. Investigation, conducting experiments, and acquiring data, V. N.D.C., Y.S., X. C., B.B.M., and B.B.S, and Writing–Review and Editing, V.N.D.C., Y.S., and B.B.S.

Ethical approval

The studies were approved by institutional IRB as well as IACUC.

Declaration of competing interest

I declare that there is no conflict of Interest.

Data availability

Data will be made available on request.

Acknowledgments

This work was funded by grant support from the NIDCR/ NIH (R01DE017102; R01DE022765) awarded to B.B.S. The funders had no further role in study design, data analysis, and/or interpretation of the data. Flow Cytometry Facility is supported by UTHSCSA, NIH-NCI P30 CA054174-20 and UL1 TR001120.

Appendix A. Supplementary data

Supplementary data to this article can be found online at https://doi.org/10.1016/j.jtauto.2023.100210.

References

[1] M. Teruel, et al., Integrative epigenomics in Sjogren s syndrome reveals novel pathways and a strong interaction between the HLA, autoantibodies and the interferon signature, Sci. Rep. 11 (1) (2021), 23292.
[2] R.I. Fox, Sjogren's syndrome, Lancet 366 (9482) (2005) 321–331.
[3] F. Andre, B.C. Bockle, Sjogren's syndrome, J Dtsch Dermatol Ges 20 (7) (2022) 980–1002.
[4] J. Kim, Y.S. Kim, S.H. Park, Metformin as a treatment strategy for Sjogren's syndrome, Int. J. Mol. Sci. 22 (13) (2021).
[5] G. Rena, D.G. Hardie, E.R. Pearson, The mechanisms of action of metformin, Diabetologia 60 (9) (2017) 1577–1585.
[6] G. Zhou, et al., Role of AMP-activated protein kinase in mechanism of metformin action, J. Clin. Invest. 108 (8) (2001) 1167–1174.
[7] A.K. Madiraju, et al., Metformin suppresses gluconeogenesis by inhibiting mitochondrial glycerophosphate dehydrogenase, Nature 510 (7506) (2014) 542–546.
[8] J. Kiripolsky, L.G. McCabe, J.M. Kramer, Innate immunity in Sjogren's syndrome, Clin. Immunol. 182 (2017) 4–13.
[9] S. Veenbergen, A. Kozmar, P.L.A. van Daele, M.W.J. Schreurs, Autoantibodies in Sjogren's syndrome and its classification criteria, J. Transl. Autoimmun 5 (2022), 100138.
[10] Z. Zhang, et al., Metformin enhances the antitumor activity of CD8(+) T lymphocytes via the AMPK-miR-107-eomes-PD-1 pathway, J. Immunol. 204 (9) (2020) 2575–2588.
[11] F. Ursini, et al., Metformin and autoimmunity: a "new deal" of an old drug, Front. Immunol. 9 (2018) 1236.
[12] J.W. Kim, et al., Metformin improves salivary gland inflammation and hypofunction in murine Sjogren's syndrome, Arthritis Res. Ther. 21 (1) (2019) 136.
[13] C.Y. Wang, et al., Metformin use was associated with reduced risk of incidental Sjogren's syndrome in patients with type 2 diabetes: a population-based cohort study, Front. Med. 8 (2021), 796615.
[14] M.T. Kasaian, H. Ikematsu, P. Casali, Identification and analysis of a novel human surface CD5- B lymphocyte subset producing natural antibodies, J. Immunol. 148 (9) (1992) 2690–2702.
[15] L. Shen, et al., Development of autoimmunity in IL-14alpha-transgenic mice, J. Immunol. 177 (8) (2006) 5676–5686.
[16] L. Shen, et al., IL-14 alpha, the nexus for primary Sjogren's disease in mice and humans, Clin. Immunol. 130 (3) (2009) 304–312.
[17] L. Shen, et al., A role for lymphotoxin in primary Sjogren's disease, J. Immunol. 185 (10) (2010) 6355–6363.
[18] L.Y. Teos, et al., IP3R deficit underlies loss of salivary fluid secretion in Sjogren's Syndrome, Sci. Rep. 5 (2015), 13953.
[19] T. Kondo, H. Muragishi, M. Imaizumi, A cell line from a human salivary gland mixed tumor, Cancer 27 (2) (1971) 403–410.
[20] S. Parasuraman, R. Raveendran, R. Kesavan, Blood sample collection in small laboratory animals, J. Pharmacol. Pharmacother. 1 (2) (2010) 87–93.
[21] M.I. Christodoulou, E.K. Kapsogeorgou, H.M. Moutsopoulos, Characteristics of the minor salivary gland infiltrates in Sjogren's syndrome, J. Autoimmun. 34 (4) (2010) 400–407.
[22] S.S. Kassan, H.M. Moutsopoulos, Clinical manifestations and early diagnosis of Sjogren syndrome, Arch. Intern. Med. 164 (12) (2004) 1275–1284.
[23] R. Liao, et al., Recent advances of salivary gland biopsy in Sjogren's syndrome, Front. Med. 8 (2021), 792593.
[24] H.M. Ibrahem, B cell dysregulation in primary Sjogren's syndrome: a review, Jpn Dent Sci Rev 55 (1) (2019) 139–144.
[25] A. Hansen, P.E. Lipsky, T. Dorner, B cells in Sjogren's syndrome: indications for disturbed selection and differentiation in ectopic lymphoid tissue, Arthritis Res. Ther. 9 (4) (2007) 218.
[26] H. Jiang, et al., Metformin plays an antitumor role by downregulating inhibitory cells and immune checkpoint molecules while activating protective immune responses in breast cancer, Int. Immunopharm. 118 (2023), 110038.
[27] D.E. Clapham, Calcium signaling, Cell 131 (6) (2007) 1047–1058.
[28] M. Vig, J.P. Kinet, Calcium signaling in immune cells, Nat. Immunol. 10 (1) (2009) 21–27.
[29] V. Nascimento Da Conceicao, et al., Resolving macrophage polarization through distinct Ca(2+) entry channel that maintains intracellular signaling and mitochondrial bioenergetics, iScience 24 (11) (2021), 103339.
[30] P. Sukumaran, A. Schaar, Y. Sun, B.B. Singh, Functional role of TRP channels in modulating ER stress and Autophagy, Cell Calcium 60 (2) (2016) 123–132.
[31] P. Sukumaran, et al., TRPC1 expression and function inhibit ER stress and cell death in salivary gland cells, FASEB Bioadv 1 (1) (2019) 40–50.
[32] A. Andersohn, et al., Aggregated and hyperstable damage-associated molecular patterns are released during ER stress to modulate immune function, Front. Cell Dev. Biol. 7 (2019) 198.
[33] Y. Sun, et al., Targeting alarmin release reverses Sjogren's syndrome phenotype by revitalizing Ca(2+) signalling, Clin. Transl. Med. 13 (4) (2023) e1228.
[34] J. Zhang, et al., Endoplasmic reticulum stress-mediated cell death in liver injury, Cell Death Dis. 13 (12) (2022) 1051.
[35] M. Ramos-Casals, P. Brito-Zeron, A. Siso-Almirall, X. Bosch, Primary sjogren syndrome, BMJ 344 (2012) e3821.
[36] O.D. Konsta, et al., Defective DNA methylation in salivary gland epithelial acini from patients with Sjogren's syndrome is associated with SSB gene expression, anti-SSB/LA detection, and lymphocyte infiltration, J. Autoimmun. 68 (2016) 30–38.
[37] T. Guerrier, et al., Role of Toll-like receptors in primary Sjogren's syndrome with a special emphasis on B-cell maturation within exocrine tissues, J. Autoimmun. 39 (1–2) (2012) 69–76.
[38] J.A. Chiorini, D. Cihakova, C.E. Ouellette, P. Caturegli, Sjogren syndrome: advances in the pathogenesis from animal models, J. Autoimmun. 33 (3–4) (2009) 190–196.
[39] P.L. Cohen, A. McCulloch, Fingolimod reduces salivary infiltrates and increases salivary secretion in a murine Sjogren's model, J. Autoimmun. 115 (2020), 102549.
[40] S. Selvaraj, et al., Neurotoxin-induced ER stress in mouse dopaminergic neurons involves downregulation of TRPC1 and inhibition of AKT/mTOR signaling, J. Clin. Invest. 122 (4) (2012) 1354–1367.
[41] B.B. Singh, et al., Calmodulin regulates Ca(2+)-dependent feedback inhibition of store-operated Ca(2+) influx by interaction with a site in the C terminus of TrpC1, Mol. Cell 9 (4) (2002) 739–750.
[42] B.B. Singh, et al., Trp1-dependent enhancement of salivary gland fluid secretion: role of store-operated calcium entry, FASEB J 15 (9) (2001) 1652–1654.
[43] X. Liu, et al., Attenuation of store-operated Ca2+ current impairs salivary gland fluid secretion in TRPC1(-/-) mice, Proc. Natl. Acad. Sci. U.S.A. 104 (44) (2007) 17542–17547.
[44] B. Ming, Y. Zhu, J. Zhong, L. Dong, Immunopathogenesis of Sjogren's syndrome: current state of DAMPs, Semin. Arthritis Rheum. 56 (2022), 152062.